The effects of plaque morphology and material properties on peak cap stress in human coronary arteries

Akyildiz, AC; Speelman, L; Nieuwstadt, HA; van Brummelen, H; Virmani, R; van der Lugt, A.; van der Steen, AFW; Wentzel, JJ; Gijsen, FJH

DOI
10.1080/10255842.2015.1062091

Publication date
2016

Document Version
Final published version

Published in
Computer Methods in Biomechanics and Biomedical Engineering

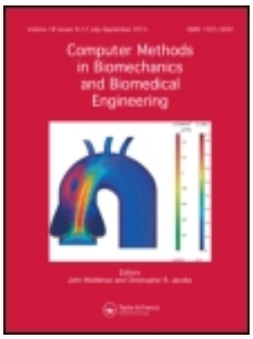

Computer Methods in Biomechanics and Biomedical Engineering

ISSN: 1025-5842 (Print) 1476-8259 (Online) Journal homepage: www.tandfonline.com/journals/gcmb20

The effects of plaque morphology and material properties on peak cap stress in human coronary arteries

Ali C. Akyildiz, Lambert Speelman, Harm A. Nieuwstadt, Harald van Brummelen, Renu Virmani, Aad van der Lugt, Anton F.W. van der Steen, Jolanda J. Wentzel & Frank J.H. Gijsen

To cite this article: Ali C. Akyildiz, Lambert Speelman, Harm A. Nieuwstadt, Harald van Brummelen, Renu Virmani, Aad van der Lugt, Anton F.W. van der Steen, Jolanda J. Wentzel & Frank J.H. Gijsen (2016) The effects of plaque morphology and material properties on peak cap stress in human coronary arteries, Computer Methods in Biomechanics and Biomedical Engineering, 19:7, 771-779, DOI: 10.1080/10255842.2015.1062091

To link to this article: https://doi.org/10.1080/10255842.2015.1062091

Published online: 03 Aug 2015.

Computer Methods in Biomechanics and Biomedical Engineering, 2016
Vol. 19, No. 7, 771–779, http://dx.doi.org/10.1080/10255842.2015.1062091

Taylor & Francis
Taylor & Francis Group

The effects of plaque morphology and material properties on peak cap stress in human coronary arteries

Ali C. Akyildiz[a1], Lambert Speelman[a,b], Harm A. Nieuwstadt[a], Harald van Brummelen[c,d], Renu Virmani[e], Aad van der Lugt[f], Anton F.W. van der Steen[a,g], Jolanda J. Wentzel[a] and Frank J.H. Gijsen[a]*

[a]*Department of Biomedical Engineering, Thoraxcenter, Erasmus Medical Center, Rotterdam, The Netherlands;* [b]*Interuniversity Cardiology Institute of the Netherlands (ICIN), Utrecht, The Netherlands;* [c]*Department of Mechanical Engineering, Eindhoven University of Technology, Eindhoven, The Netherlands;* [d]*Department of Mathematics and Computer Science, Eindhoven University of Technology, Eindhoven, The Netherlands;* [e]*CVPath Institute, Inc., Gaithersburg, MD, USA;* [f]*Department of Radiology, Erasmus Medical Center, Rotterdam, The Netherlands;* [g]*Department of Applied Sciences, Delft University of Technology, Delft,The Netherlands*

(*Received 12 November 2014; accepted 10 June 2015*)

Heart attacks are often caused by rupture of caps of atherosclerotic plaques in coronary arteries. Cap rupture occurs when cap stress exceeds cap strength. We investigated the effects of plaque morphology and material properties on cap stress. Histological data from 77 coronary lesions were obtained and segmented. In these patient-specific cross sections, peak cap stresses were computed by using finite element analyses. The finite element analyses were 2D, assumed isotropic material behavior, and ignored residual stresses. To represent the wide spread in material properties, we applied soft and stiff material models for the intima. Measures of geometric plaque features for all lesions were determined and their relations to peak cap stress were examined using regression analyses. Patient-specific geometrical plaque features greatly influence peak cap stresses. Especially, local irregularities in lumen and necrotic core shape as well as a thin intima layer near the shoulder of the plaque induce local stress maxima. For stiff models, cap stress increased with decreasing cap thickness and increasing lumen radius ($R = 0.79$). For soft models, this relationship changed: increasing lumen radius and increasing lumen curvature were associated with increased cap stress ($R = 0.66$). The results of this study imply that not only accurate assessment of plaque geometry, but also of intima properties is essential for cap stress analyses in atherosclerotic plaques in human coronary arteries.

Keywords: atherosclerosis; cap stress; plaque morphology; plaque properties; finite element models

Introduction

Among the cardiovascular diseases, the top two causes on the mortality list are stroke and coronary heart disease. More than 70% of fatal heart attacks are caused by the rupture of atherosclerotic plaques in coronaries (Falk 2006). A correct stratification is essential in order to distinguish rupture prone vulnerable plaques (which would need surgical treatment) from stable plaques. Post-mortem studies have shown that a thin cap and a large lipid rich necrotic core (NC) are common morphological features of vulnerable plaques (Falk 2006). However, not all plaques with such morphological features rupture (Virmani et al. 2006). This calls for a further exploration of markers for plaque vulnerability.

A plaque cap ruptures when the local stress exceeds the cap strength. Cap stress is determined by blood pressure, plaque morphology and the material properties of plaque constituents. Idealized plaque geometries were used frequently to study the effect of plaque morphology on cap stresses. In these idealized models, it was demonstrated that thinner caps increase the peak cap stress in exponential fashion (Loree et al. 1992; Finet et al. 2004). Additionally, an increase in NC size and angle and a decrease in intima thickness behind the NC have been shown to elevate cap stresses as well (Ohayon et al. 2008; Akyildiz et al. 2011).

Only a limited number of studies investigated realistic plaque geometries. These studies either included a limited number of samples (Cheng et al. 1993; Huang et al. 2001; Chau et al. 2004; Finet et al. 2004) or assumed values for essential features like cap thickness (Ohayon et al. 2008). In a more extensive study using MRI, it was demonstrated that lumen curvature has a significant influence on peak cap stress (Teng et al. 2010), but it was recently shown that this imaging modality cannot image thin caps accurately enough for peak cap stress assessment (Nieuwstadt, Speelman, et al. 2013). In an IVUS-based study in 15 patients, Imoto et al. (2005) concluded that the influence of cap thickness on cap stress was heavily modulated by plaque shape. This implies that observations based on idealized geometries might not hold for realistic geometries.

The influence of the material properties on peak cap stresses was investigated before. In some of these studies (Loree et al. 1992; Cheng et al. 1993; Williamson et al. 2003; Maldonado et al. 2012), the variations in plaque properties were limited, leading to only minor changes in cap stresses. However, in a recent review we showed that

*Corresponding author. Email: f.gijsen@erasmusmc.nl

available experimental data indicate that the intima properties might show much more variation (Akyildiz et al. 2014). Including these variations might influence peak cap stresses much more (Ohayon et al. 2012), which was also shown to be the case in idealized coronary plaque models (Akyildiz et al. 2011). The effect of anisotropic intima behavior was evaluated in two numerical studies (Tang et al. 2009; Liang et al. 2013). The results were inconclusive as one reported effects of fibrous cap anisotropy on the peak cap stress up to 100% (Tang et al. 2009), while the other reported effects below 30% (Liang et al. 2013). The scarcity of numerical studies on this topic can be explained by absence of complete experimental data-sets that comprise the relevant parameters needed for modeling anisotropy.

The aim of the current study is threefold. The first aim was to investigate the effects of plaque geometry on cap stresses in human atherosclerotic coronaries. While in previous studies idealized plaque geometries were investigated (Akyildiz et al. 2011), the current study includes a sizeable number of realistic plaque geometries from histology images. Second, it was investigated how the effect of geometry was modulated by the properties of the intima tissue. Finally, regression analysis was applied to determine how well peak cap stresses could be modeled using geometrical plaque features alone.

Methods

Histology

Thirteen atherosclerotic coronary segments (four from the left anterior descending artery, four first diagonal branch, three from the right coronary artery, and two from the left circumflex artery), excised from seven donors post-mortem, were perfusion fixed with formalin at 100 mmHg. Cross-sections of 5 μm thickness were obtained. Movat pentachrome staining was used for histological examination. Lumen, intima, lipid rich NC, media, and adventitia were delineated on the histology images (Figure 1). In total, 55 histology cross sections with 77 NC regions were obtained.

Finite elements analysis

Two-dimensional finite element models (ABAQUS Standard 6.11.1) with large deformation formulation and plane strain assumption were generated. Since the histology images were obtained from arteries fixed at 100 mmHg, the backward incremental method (Speelman et al. 2011) was incorporated into the finite element simulations to compute the initial stresses present in the perfusion fixed plaques. In summary, using a straightforward finite element analysis, the intraluminal pressure is step-wise increased in the original geometry up to 100 mmHg. After each step, the stresses in the model are obtained and the geometry is deformed. For the next step, this deformation is discarded and the geometry is reset to its original form and the calculated stresses are added to the model as initial stress condition. At least six pressure increments were used to reach 100 mmHg and the final initial stress state. From there, a peak systolic pressure of 140 mmHg was applied (Figure 1). The stress results reported in this paper are maximum principal stresses at this systolic pressure.

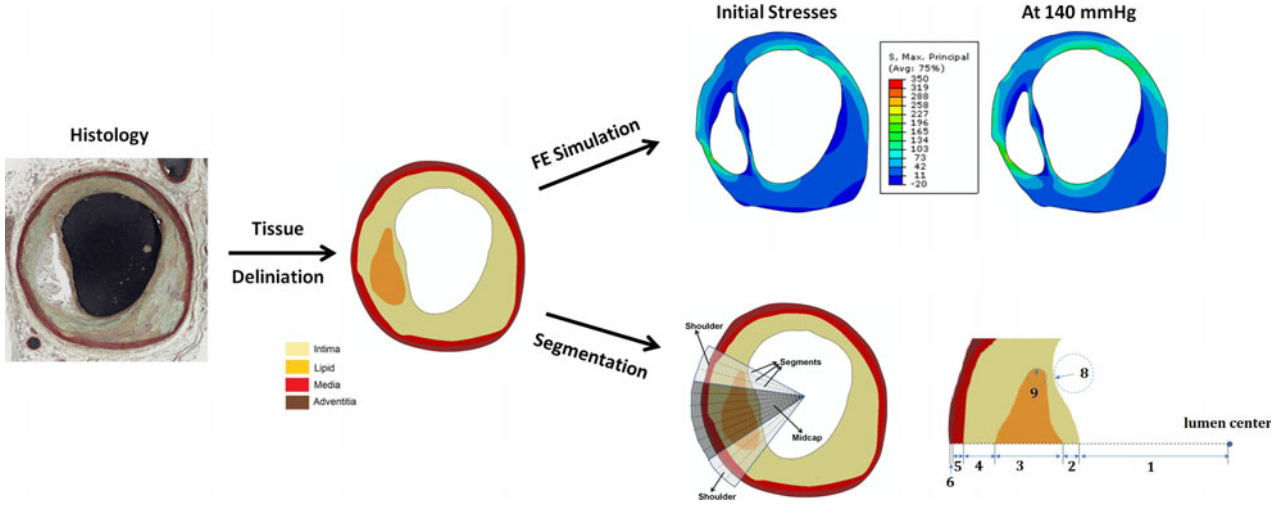

Figure 1. From histology to data analysis: first, the histological images are segmented, and the adventitia, media, intima and lipid-rich necrotic core are delineated. The delineated cross sections are converted to a finite element mesh, and the backward incremental method is applied to compute initial stresses. Finally, the maximal principal stresses at 140 mmHg are computed, and they are analysed using the segmentation based on the original delineated geometry. The geometrical parameters are illustrated in the lower right panel. The numbers correspond to (1) lumen radius, (2) cap thickness, (3) necrotic core thickness, (4) intima thickness behind the necrotic core, (5) media thickness, (6) adventitia thickness, (7) 4 + 5 + 6, (8) lumen curvature, (9) necrotic core curvature.

The nonlinear mechanical behavior of the media and adventitia was modeled by fitting incompressible, hyperelastic Yeoh models (Holzapfel 2000) to the uniaxial tension test results obtained from human coronary vessels (Holzapfel et al. 2005). The Yeoh model is characterized by a strain energy density function, W_{Yeoh}:

$$W_{\text{Yeoh}} = \sum_{i=1}^{3} C_i(\bar{I}_1 - 3)^i + \frac{1}{D_i}(J-1)^{2i}, \quad (1)$$

where $\bar{I}_1 = \bar{\lambda}_1^2 + \bar{\lambda}_2^2 + \bar{\lambda}_3^2$ is the first deviatoric strain invariant where deviatoric strains are $\bar{\lambda}_i = J^{1/3}\lambda_i$ with λ_1, λ_2 and λ_3 being the principal strains. C_i and D_i are material constants. Neo-Hookean material model (Holzapfel 2000) with a strain energy density function, W_{NH}, was employed for intima and NC. The Neo-Hookean model is a special case of the Yeoh model ($i = 1$), with only one material constant (C). For both models, incompressibility was imposed in the model for all components by setting D to 10^{-6}. Neo-Hookean material model (Holzapfel 2000) with a strain energy density function, W_{NH}, was employed for intima and NC:

$$W_{\text{NH}} = C(I_1 - 3). \quad (2)$$

The only material constant in the model is C [kPa]. For small deformations, C can be derived from the Young's modulus, E [kPa], by $C = E/6$. Intima and NC were assumed to be incompressible. As for the intima mechanical properties measurements of coronary plaques are scarce, stress computations were done with intima material models with both a relatively low (Young's modulus $= 30$ kPa) and high stiffness (1000 kPa). These values cover the range of atherosclerotic intima stiffness reported in earlier experimental studies from all vascular territories (Akyildiz et al. 2014). The values of all material constants are listed in Table 1.

Data analysis

The delineated histology cross-sections were used to identify cap areas (Figure 1). Each cap area was divided into three regions: two shoulders and one midcap. These regions were further divided into segments. The peak cap stress and nine geometric parameters were determined per cap area, region and segment. These nine geometric parameters are (1) lumen radius, (2) cap thickness, (3) NC thickness, (4) intima thickness behind the NC, (5) media thickness, (6) adventitia thickness, (7) total intima-media-adventitia thickness, (8) lumen curvature, and (9) NC curvature. The mass center of the lumen was defined as the lumen center. Lumen radius and plaque components' thicknesses were measured on the line drawn from the lumen center. Lumen and NC curvatures were calculated by inverting the radius of the osculating circle through three adjacent mesh nodes on the lumen and NC contours. The geometrical quantities are illustrated in lower right panel in Figure 1.

Table 1. Material constants of the plaque components.

Tissue	Material constants
Media	$C_1 = 6.3$ kPa, $C_2 = 25$ kPa, $C_3 = 255$ kPa
Adventitia	$C_1 = 2.4$ kPa, $C_2 = 80$ kPa, $C_3 = 345$ kPa
Intima	$C = 166$ kPa (stiff) or 5.5 kPa (soft)
NC	$C = 0.166$ kPa

An additional geometric parameter for cap area was the NC angle. An in-house written MATLAB script was used to determine maximum, minimum and mean values of the geometric parameters.

A number of plaques contained more than one NC. We only included these NCs if the edges of the NCs were clearly separated (average separation angle $= 70$ degrees). This clear separation avoided crosstalk between the NCs, and therefore they were treated separately in the analyses. Statistical analyses were performed with SPSS (release 17.0). All data (peak cap stress for the stiff and the soft models and geometric parameters) were checked for normality using Shapiro–Wilk test. Since the data were not normally distributed, nonparametric tests were employed. For multivariate regression analysis, log-transformation was used to improve the normality and the model fit. In general, a statistical significance was considered if $p < 0.001$.

Two approaches were followed during the analyses: a local and global approach. Segmental analysis aimed deepening our understanding of the influence of *local* geometric parameters on *local* peak cap stress. First, nonparametric Spearman's correlations were calculated to investigate relationships between segmental geometric parameters and peak cap stress in segments, and between segmental geometric parameters themselves. Second, a multivariate regression analysis with stepwise insertion method was performed, with local peak cap stress being the dependent variable and the geometric parameters being the independent variables. A nonparametric Mann–Whitney U test was used to compare the peak stresses and geometric parameters in the shoulder and midcap regions. For global plaque analysis, a multivariate regression analysis was employed to predict peak cap stress in a plaque cross-section using *global* geometric plaque parameters for both the stiff and the soft intima models. Standardized coefficients are reported to allow comparison the relative effects of the geometric parameters measured on different scales. Standardized coefficients describe how many standard deviations the dependent variables changes if the independent variable changes one standard deviation. Unstandardized coefficients reflect the results of regression analyses on the original data.

Table 2. Geometric parameter values for cap analysis.

Geometric parameter	Median [Q1:Q3]
Min. Cap Th.	190 [64:400] μm
Max. NC Th.	508 [297:598] μm
Min. Intima Th.	100 [47:191] μm
Min. Media Th.	63 [25:83] μm
Min. Adventitia Th.	55 [34:88] μm
Min. IMA Th.	282 [2209:422] μm
Max Lumen Radius	922 [780:1075] μm
NC Angle	55 [35:75] °
Max. Lumen Curv.	3.4 [2.6:5.8] μm^{-1}
Max. NC Curv.	31 [21:55] μm^{-1}

Note: Th, thickness; NC, necrotic core; Adv, adventitia; IMA, intima-media-adventitia; Curv, curvature.

Results

Geometrical plaque parameters

The coronary plaques investigated in the present study showed diverse geometries. Table 2 gives the median and quartile values of the most relevant geometric parameters. The minimum cap thickness had a median of 190 μm [1st quartile (Q_1):3rd quartile (Q_3) = 64:400 μm]. The maximum NC thickness had a median of 507 (297:597) μm. The median value of lumen radius was 922 (780:1075) μm.

Stress results

The finite element simulations revealed that the stress distribution and peak cap stress values strongly depended on plaque geometry. Figure 2(A)–(C) illustrates how stress results for the stiff intima models were influenced by distinct geometrical plaque features. In Figure 2(A), a representative example of a plaque with a smooth NC and a smooth lumen shape is shown. For this type of plaques, peak stresses in the shoulders were mostly at the lumen border (140 and 120 kPa in the representative example in Figure 2(A)). In the midcap region, peak stress was present at the NC border (230 kPa in Figure 2(A)). Moreover, lowest stresses in the entire cap were at the luminal side in the midcap region (10 kPa in Figure 2(A)). The effect of lumen irregularities is illustrated in Figure 2(B). Locally increased lumen curvature correlate strongly with peak stress locations (91 kPa in Figure 2(B)). Figure 2(C) illustrates that for plaques with irregular NC shape, peak stress locations shift toward the irregularities (210 kPa at the luminal side and 305 kPa at the NC border in Figure 2 (C)). Figure 2(D) demonstrates that a thin intima layer in the nondiseased part of a vessel adjacent to the cap shoulder showed high stresses (475 kPa in Figure 2(D)) and increased the stresses within the cap shoulder. The peak cap stress for the soft intima models was lower when compared to the stiff intima models (stiff model: median [Q1:Q3] = 135 [93:229] kPa; soft model: 96 [46:168] kPa,

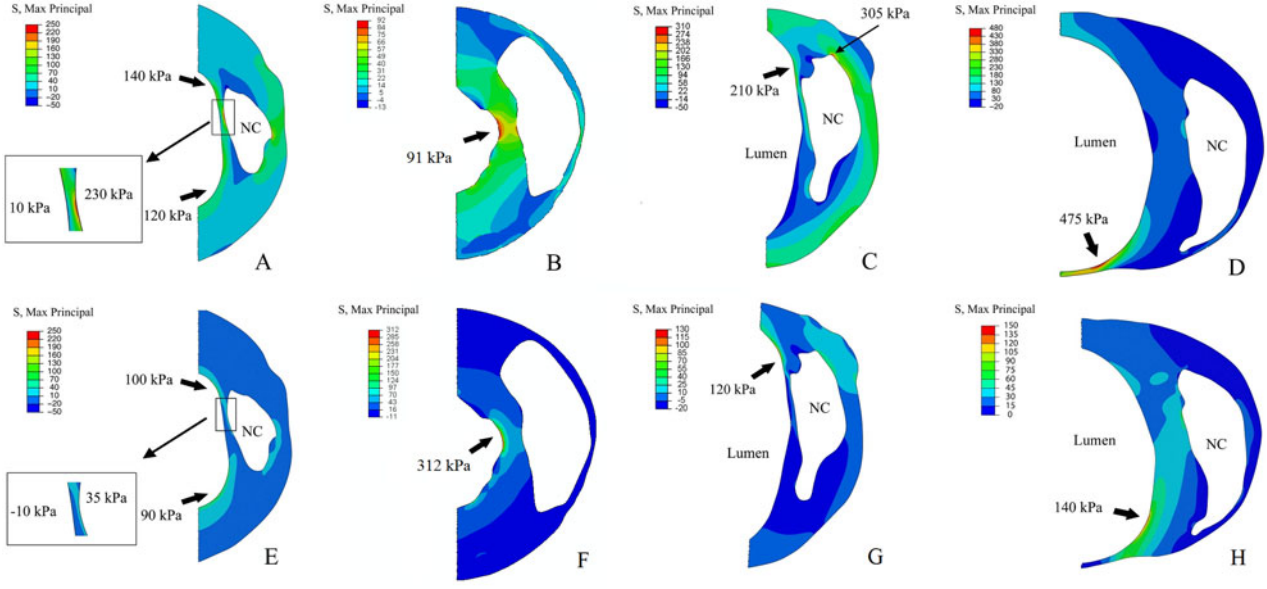

Figure 2. Finite elements analysis results showing maximum principal stress (in kPa) within the intima of atherosclerotic coronary plaques. The results for the stiff models are depicted in panels A–D, for the soft models in panels E–H. (A) In plaques with smooth lumen and NC shapes, higher stresses were observable at the lumen border in the shoulders and at the NC border in the midcap area. Very low, even negative stresses were present at the lumen border in midcap. (B) Irregularities on the lumen or (C) NC border caused stress concentrations. (D) High stresses occurred in the thin intima region adjacent to plaque shoulder and increased the cap stresses. Qualitatively, the soft models (panels E–H) show comparable results, although the peak stresses at the NC side and the effect of local lumen curvature is more pronounced.

$p = 0.02$). Overall, the results for the soft model showed similar dependencies of cap stress on the geometrical plaque features as for the stiff intima models. However, the peak cap stresses at the NC side were markedly lower (35 kPa in Figure 2(E)) and the effect of local lumen curvature was more pronounced (312 kPa in Figure 2(F)). Local peak stress in the shoulder region (stiff model: median [Q1:Q3] = 88 [49:176] kPa, soft model: median [Q1:Q3] = 51 [17:109] kPa) and midcap region (stiff model: median [Q1:Q3] = 102 [65:172] kPa; soft model: median [Q1:Q3] = 35 [12:73] kPa) was not significantly different.

Local regression analysis

The relationships between local peak cap stress and the geometric parameters on segmental basis were investigated to gain better insight of the effect of geometry on peak cap stress. For the stiff models, segmental bivariate analysis revealed that four geometric plaque parameters significantly correlated to local peak cap stress: minimum cap thickness, minimum media thickness, maximum lumen curvature, and maximum lumen radius (Table 3). Minimum cap thickness showed a strong, negative correlation ($\rho = -0.59$) to stress. Another strong correlation was observed for maximum lumen radius in with a positive trend ($\rho = 0.47$). Maximum lumen curvature ($\rho = 0.17$) and minimum media thickness ($\rho = 0.14$) were positively correlated to local peak cap stress. For the soft models, geometrical irregularities were correlated strongest to peak cap stress: maximum lumen curvature and maximum NC curvature were positively correlated with $\rho = 0.50$ and $\rho = 0.20$, respectively. Cap thickness and maximum lumen radius were also significantly correlated with peak cap stress, but much weaker ($\rho = -0.17$ and $\rho = 0.13$, respectively). The minimum media thickness and the minimum total intima-media-adventitia thickness were also (weakly) correlated to peak stresses in the soft models. Surprisingly, maximum NC thickness did not show a significant correlation to peak cap stress for both models.

There were correlations between the geometric plaque parameters indicating that the influence of one geometric feature might be confounded by another one. Therefore, we performed multivariate regression analysis on segmental results. Using backward elimination method, a model with three geometric plaque parameters was obtained (Table 4). For the stiff models, the multivariate regression (R-value = 0.69) showed that thinner cap elevated the local peak stress, and smaller lumen radius and lumen curvature decreased the peak stress. For the soft models, increasing lumen curvature and lumen radius increased peak stress, while increasing the media thickness decreased peak stress (R-value = 0.55).

Global regression analysis

Multivariate regression analysis was employed to predict the global peak cap stress in plaques from the geometrical parameters. For the stiff models, minimum cap thickness and

Table 3. Nonparametric Spearman's correlation coefficients for segmental analysis.

	Min Cap Th.	Max NC Th.	Min Intima Th.	Min Media Th.	Min Adv. Th.	Min IMA Th.	Max Lumen Curv.	Max NC Curv.	Max Lumen Rad.
Peak segment stress (stiff)	−0.59*	0.01	0.06	0.14*	−0.07	0.09	0.17*	0.09	0.47*
Peak segment stress (soft)	−0.17*	0.06	0.08	−0.12*	0.11	0.12*	0.50*	0.20*	0.13*

Note: All parameters are log-transformed. Th, thickness; NC, necrotic core; Adv, adventitia; IMA, intima-media-adventitia; Curv, curvature. Asterisk indicates significant correlation ($p < 0.001$).

Table 4. Multivariate regression model for segmental analysis.

	Stiff model: log(PeakCapStress)			Soft model: log(PeakCapStress)		
	UC	95% CI	SC	UC	95% CI	SC
Constant	1.20	[0.78;1.62]		2.73	[1.74; −3.72]	
log(MinCapTh)	−0.59	[−0.64; −0.53]	−0.57	–	–	–
log(MaxLumenRadius)	0.87	[0.74;1.00]	0.35	0.52	[0.20;0.84]	0.15
log(MaxLumenCurv)	0.15	[0.10;0.21]	0.15	0.71	[0.58;0.84]	0.49
log(MinMediaTh)	–	–	–	−0.40	[−0.59; −0.21]	−0.19

Note: Peak cap stress is in kPa, minimum cap thickness and maximum lumen radius are in μm. UC, unstandardized coefficient; CI, confidence interval; SC, standardized coefficient. For the stiff model, $R = 0.69$ and for the soft model, $R = 0.55$. p-Values for the terms are <0.001.

maximum lumen radius were the only significant geometric parameters in the final statistical model ($R = 0.79$):

$$\log(\text{PeakCapStress}) = 0.97 - 0.41 \times \log(\text{MinCapTh}) + 0.71 \times \log(\text{MaxLumenRadius})$$

with peak cap stress in kPa, minimum cap thickness and maximum lumen radius in μm. A thinner cap and larger maximum lumen radius increased the peak cap stress in a plaque. Lumen curvature, which was one of the important parameters in the local multivariate analysis, did not have a significant effect in global analysis. For the soft intima models, only maximum lumen radius and maximum lumen curvature significant contributed to peak cap stress ($R = 0.66$):

$$\log(\text{PeakCapStress}) = 2.52 + 0.68 \times \log(\text{MaxLumenRadius}) + 1.09 \times \log(\text{MaxLumenCurv})$$

Table 5 shows the standardized and unstandardized coefficients and statistical significance of the geometric parameters.

Figure 3 illustrates the results of the global regression analyses. Figure 3(A) illustrates the strong non-linear dependency of the peak cap stress on cap thickness and the weaker more linear relationship with the lumen radius for the stiff models. Figure 3(B) shows how the peak cap for the soft models depends on lumen curvature and lumen radius.

Discussion

This study focused on the impact of realistic plaque geometries on computed peak cap stresses in atherosclerotic plaques. To our best knowledge, this is the first study to investigate this topic in a sizeable group of 77 NCs, using high-resolution histological data as input. The geometrical plaque features in this study cover a great variation in cap thickness and NC size, including typical *in vivo* shape irregularities. These irregularities, not present in studies that focus on idealized geometries, greatly influence the stress distribution in coronary plaques, inducing local peak stresses. On top of these irregularities, also the presence of a thin intima layer, adjacent to the shoulder of the plaque, leads to stress concentrations.

When considering the influence of geometrical parameters on local cap stresses for the stiff models, this

Table 5. Multivariate regression model for cap analysis.

	Stiff model: log(PeakCapStress)			Soft model: log(PeakCapStress)		
	UC	95% CI	SC	UC	95% CI	SC
Constant	0.97	[0.02; 1.92]		2.52	[0.61; 4.45]	
log(MinCapTh)	−0.41	[−0.50; −0.32]	−0.67	–	–	–
log(MaxLumenRadius)	0.71	[0.40; 1.02]	0.34	0.68	[0.03; 1.34]	0.18
log(MaxLumenCurv)	–	–	–	1.09	[0.81; 1.37]	0.68

Note: p-Values for the terms are <0.001. Peak cap stress is in kPa, minimum cap thickness and maximum lumen radius are in μm. UC, unstandardized coefficient; CI, confidence interval; SC, standardized coefficient. For the stiff model, $R = 0.79$ and for the soft model, $R = 0.67$.

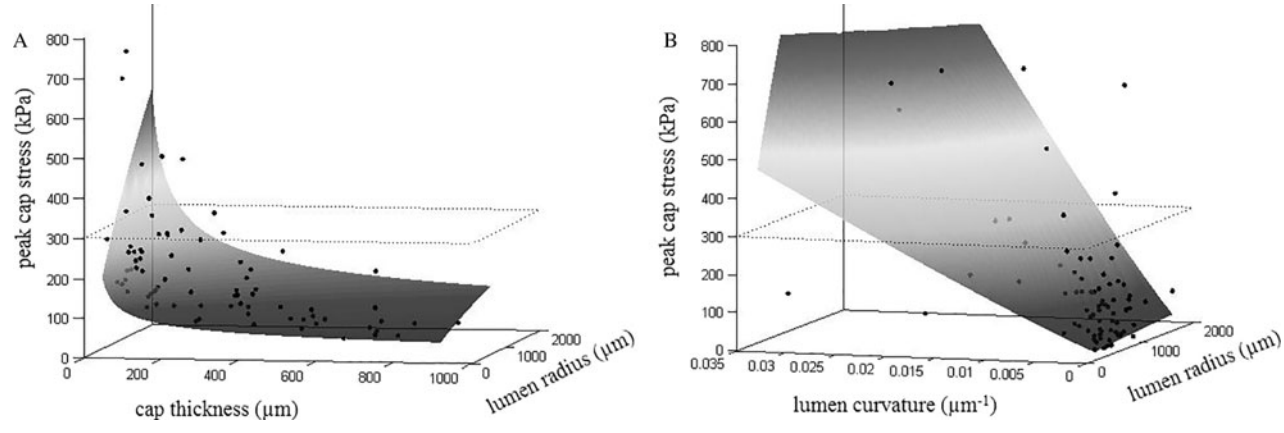

Figure 3. Panel A shows the 3D representation of the regression analyses for the stiff model, clearly showing the strong non-linear dependency of peak cap stress on cap thickness and the weaker near linear dependency on lumen radius. For the soft models (panel B), the dependency of peak cap stress on lumen curvature and radius is shown.

study confirms the dominant effect of cap thickness on cap stress (Ohayon et al. 2008; Akyildiz et al. 2011). However, this study also demonstrates that there are marked differences, induced by the combined effect of the aforementioned plaque specific features. Most notably, *necrotic core thickness* has been shown to be an important factor in idealized geometries for cap stresses (Ohayon et al. 2008; Akyildiz et al. 2011). However, in the present study in realistic geometries, no significant effect of NC thickness on peak cap stress was found. It was also shown that high l*ocal lumen curvature*, which indicates an irregularity on lumen shape, increases the local stresses in coronary artery plaques. Optical coherence tomography images demonstrate that these irregularities are frequently observed in patients (Tearney et al. 2012) and might therefore be an important geometrical surrogate for peak stresses in coronary plaques. Teng et al. (2010) reached a similar conclusion for the effect of lumen irregularities in carotid plaques, using finite element models based on MRI. Since MRI-based segmentation tends to smoothen out local irregularities (Nieuwstadt, Geraedts, et al. 2013), the effect might even be stronger than reported in that study. *Maximum lumen radius* was another important factor for local peak cap stress and in line with the Laplace Law, larger radius elevated the stress. When comparing plaques with similar cap thickness in the proximal part (with larger lumen radius) to plaques in the distal part of the coronary tree (with a smaller lumen radius), the stress in the cap in the proximal plaque will be higher. These elevated stresses might contribute to the more frequent occurrence of plaque rupture in the proximal part of the coronary tree (von Birgelen et al. 2001). In a recent study, we investigated the influence of the plaque structures behind the NC using idealized plaque geometries and showed that media and adventitia had almost no influence, whereas a thicker intima behind the NC slightly reduced cap stress (Akyildiz et al. 2011). The results of the present study confirmed our earlier findings.

Some of the significant effects of various geometrical plaque features on local cap stresses disappear when multivariate analysis is carried out to relate global plaque features to peak cap stresses. For the stiff intima models, only minimum cap thickness and maximum lumen radius are independent predictors of cap stress. A thin cap and a large lumen radius are surrogate markers for high cap stresses, together accounting for 62% of the variation in peak cap stress. Although there is much room for improvement, these geometrical plaque features might serve as an alternative to finite elements analysis for peak cap stress prediction in a clinical setting, since both cap thickness and lumen radius can be measured directly by invasive imaging techniques, including optical coherence tomography.

Apart from the large influence of a realistic geometry on cap stresses in coronary arteries, the current study also demonstrates the importance of selecting the appropriate material model for the intima. While most numerical studies employ stiff material models (Holzapfel et al. 2014), often based on the experimental data on hypocellular aortic plaque tissue, it was recently demonstrated that these properties might overestimate stiffness of the intima in carotid and coronary plaques (Chai et al. 2014). We employed lower stiffness values from those studies in our soft model, and demonstrated that not only the overall stress levels decrease, but that the relationship between the geometrical plaque features and cap stresses change rather dramatically. For the local cap stresses, the aforementioned irregularities gain importance, especially at the expense of cap thickness. This can be explained by the fact that the impact of cap thickness on cap stress will naturally diminish if the intima is softer and closer to the properties of the NC. In the limiting case that the material properties are identical, the influence of cap thickness will disappear altogether. The predictive value of global plaque features decreases, with lumen curvature and lumen radius predicting approximately 44% of peak cap stress. These findings emphasize the importance of application of the appropriate plaque-specific material properties in patient-specific numerical studies. These properties can potentially be obtained by combining finite element models with strain imaging with ultrasound (Baldewsing et al. 2004) or MRI (Franquet et al. 2011; Nederveen et al. 2014).

For rupture risk assessment, cap strength is as important as cap stress. Strength in itself is not directly influenced by plaque morphology. However, an association between cap strength and morphology might be present. Macrophages are known to reduce cap strength (Lendon et al. 1991) and they are mainly located around the NC, with a slight prevalence for accumulating in the shoulder regions of the plaque (Davies et al. 1993). The shoulder regions of the plaque might therefore be less strong.

This study has some limitations. The number of patients the plaques were taken from is limited. However, taken the wide variation of NC features in this study into account, it can be expected that the main findings will not change when the database would have contained more patients. The intima of the investigated plaques was modeled with a rather simple homogeneous material model. Although diseased intima generally contains an accumulation of collagen fibers, the used material model did not incorporate anisotropy. The experimental data on the potential anisotropy of coronary intima tissue is to the best knowledge of the authors not available. In a recent study on carotid intima tissue, it was shown that the fiber dispersion angle was relatively wide, indicating that carotid intima tissue might be modeled with an isotropic model (Chai et al. 2013). Whether this also holds for coronary intima tissue needs to be investigated. The anisotropic material properties of media and adventitia

available in literature were not employed in the finite element computations, as the 2D simulations with initial stress analysis did not support the use of anisotropic material models. However, by approximating the mechanical behavior of the outer layers using an isotropic material model, it is assumed that the effect of this limitation is minimal in this geometrical analysis study. Residual stresses were not included in this study. Although recently some interesting approaches were introduced to assess residual stresses in atherosclerotic plaques (Riou et al. 2014; Schroder and Brinkhues 2014), there is still quite some debate on how to determine them adequately. The relevance of residual stresses for plaque mechanics was recently addressed (Holzapfel et al. 2014), and in that review it was concluded residual stresses might reduce peak cap stress and are therefore potentially relevant for rupture risk prediction. Since this study explores the effect of geometry and material properties on cap stress, we believe that ignoring the residual stresses in this study will not influence our main findings. Calcifications could not be retained due to the histological processing that was applied. Although the stabilizing effect of macro-calcifications has been shown (Huang et al. 2001), indicating that plaques without calcification might be more of vulnerable type, micro-calcification may cause stress concentrations (Vengrenyuk et al. 2008). This warrants further investigation. The analyses presented in this study are based on 2D plane strain analysis, while the arteries are 3D structures. In a previous study, we have shown that including 3D geometry in the simulations does influence absolute stress values. The difference in absolute peak cap stress values between 2D and 3D analyses were shown to be as large as 25%. However, it was also demonstrated that the relationship between geometrical features and cap stresses were largely unaltered in the 2D simulations (Nieuwstadt et al. 2012). However, another study demonstrated that there is a distinct difference in peak cap stress when comparing 2D and 3D simulations study (Balzani et al. 2012). This topic requires further research. Since anisotropy, the residual stress, and the 3D geometry were not included in this study, the absolute peak cap stress values should be interpreted with caution, especially in the context of rupture risk analyses.

In conclusion, this comparative study showed that patient-specific geometrical plaque features greatly influence peak cap stresses. Especially, local irregularities in lumen and NC shape as well as a thin intima layer near the shoulder of the plaque induce local stress maxima. These irregularities are not included in idealized plaque models and are responsible for the fact that well-established geometrical surrogates for peak cap stresses in idealized models lose their predictive value. Moreover, the choice for material properties for the intima determines how geometry influences peak cap stresses. This implies that not only accurate assessment of plaque geometry, but also of intima properties is essential for cap stress analyses in atherosclerotic plaques in human coronary arteries. The effect of anisotropy, 3D geometry, and residual stresses on absolute cap stress assessment, especially relevant in for rupture risk assessment, warrants further investigations.

Disclosure statement

No potential conflict of interest was reported by the authors.

Note

1. Current address: Department of Mechanical, Aerospace and Nuclear Engineering, Rensselaer Polytechnic Institute, Troy, MI, USA

References

Akyildiz AC, Speelman L, Gijsen FJ. 2014. Mechanical properties of human atherosclerotic intima tissue. J Biomech. 47:773–783. Epub 2014/02/18.

Akyildiz AC, Speelman L, van Brummelen H, Gutierrez MA, Virmani R, van der Lugt A, van der Steen AF, Wentzel JJ, Gijsen FJ. 2011. Effects of intima stiffness and plaque morphology on peak cap stress. Biomed Eng Online. 10:25. Epub 2011/04/12.

Baldewsing RA, de Korte CL, Schaar JA, Mastik F, van der Steen AF. 2004. A finite element model for performing intravascular ultrasound elastography of human atherosclerotic coronary arteries. Ultrasound Med Biol. 30:803–813. Epub 2004/06/29.

Balzani D, Bose D, Brands D, Erbel R, Klawonn A, Rheinbach O, Schroder J. 2012. Parallel simulation of patient-specific atherosclerotic arteries for the enhancement of intravascular ultrasound diagnostics. Eng Comput. 29:888–906.

Chai CK, Akyildiz AC, Speelman L, Gijsen FJ, Oomens CW, van Sambeek MR, van der Lugt A, Baaijens FP. 2013. Local axial compressive mechanical properties of human carotid atherosclerotic plaques-characterisation by indentation test and inverse finite element analysis. J Biomech. 46:1759–1766. Epub 2013/05/15.

Chai CK, Speelman L, Oomens CW, Baaijens FP. 2014. Compressive mechanical properties of atherosclerotic plaques–indentation test to characterise the local anisotropic behaviour. J Biomech. 47:784–792. Epub 2014/02/01.

Chau AH, Chan RC, Shishkov M, MacNeill B, Iftimia N, Tearney GJ, Kamm RD, Bouma BE, Kaazempur-Mofrad MR. 2004. Mechanical analysis of atherosclerotic plaques based on optical coherence tomography. Ann Biomed Eng. 32:1494–1503. Epub 2005/01/08.

Cheng GC, Loree HM, Kamm RD, Fishbein MC, Lee RT. 1993. Distribution of circumferential stress in ruptured and stable atherosclerotic lesions. A structural analysis with histopathological correlation. Circulation. 87:1179–1187. Epub 1993/04/01.

Davies MJ, Richardson PD, Woolf N, Katz DR, Mann J. 1993. Risk of thrombosis in human atherosclerotic plaques: role of extracellular lipid, macrophage, and smooth muscle cell content. Br Heart J. 69:377–381. Epub 1993/05/01.

Falk E. 2006. Pathogenesis of atherosclerosis. J Am Coll Cardiol. 47:C7–C12. Epub 2006/04/25.

Finet G, Ohayon J, Rioufol G. 2004. Biomechanical interaction between cap thickness, lipid core composition and blood pressure in vulnerable coronary plaque: impact on stability or instability. Coron Artery Dis. 15:13–20. Epub 2004/06/18.

Franquet A, Avril S, Le Riche R, Badel P. 2011. Identification of heterogeneous elastic properties in stenosed arteries: a numerical plane strain study. Comput Methods Biomech Biomed Eng. 15:49–58. Epub 2011/05/25.

Holzapfel GA. 2000. Nonlinear solid mechanics: a continuum approach for engineering. Chichester; New York: Wiley.

Holzapfel GA, Mulvihill JJ, Cunnane EM, Walsh MT. 2014. Computational approaches for analyzing the mechanics of atherosclerotic plaques: a review. J Biomech. 47:859–869. Epub 2014/02/05.

Holzapfel GA, Sommer G, Gasser CT, Regitnig P. 2005. Determination of layer-specific mechanical properties of human coronary arteries with nonatherosclerotic intimal thickening and related constitutive modeling. Am J Physiol Heart C. 289:H2048–H2058.

Huang H, Virmani R, Younis H, Burke AP, Kamm RD, Lee RT. 2001. The impact of calcification on the biomechanical stability of atherosclerotic plaques. Circulation. 103:1051–1056. Epub 2001/02/27.

Imoto K, Hiro T, Fujii T, Murashige A, Fukumoto Y, Hashimoto G, Okamura T, Yamada J, Mori K, Matsuzaki M. 2005. Longitudinal structural determinants of atherosclerotic plaque vulnerability: a computational analysis of stress distribution using vessel models and three-dimensional intravascular ultrasound imaging. J Am Coll Cardiol. 46:1507–1515. Epub 2001/02/27.

Lendon CL, Davies MJ, Born GV, Richardson PD. 1991. Atherosclerotic plaque caps are locally weakened when macrophages density is increased. Atherosclerosis. 87:87–90. Epub 1991/03/01.

Liang X, Xenos M, Alemu Y, Rambhia SH, Lavi I, Kornowski R, Gruberg L, Fuchs S, Einav S, Bluestein D. 2013. Biomechanical factors in coronary vulnerable plaque risk of rupture: intravascular ultrasound-based patient-specific fluid–structure interaction studies. Coron Artery Dis. 24:75–87. Epub 2013/02/01.

Loree HM, Kamm RD, Stringfellow RG, Lee RT. 1992. Effects of fibrous cap thickness on peak circumferential stress in model atherosclerotic vessels. Circ Res. 71:850–858. Epub 1992/10/01.

Maldonado N, Kelly-Arnold A, Vengrenyuk Y, Laudier D, Fallon JT, Virmani R, Cardoso L, Weinbaum S. 2012. A mechanistic analysis of the role of microcalcifications in atherosclerotic plaque stability: potential implications for plaque rupture. Am J Physiol Heart Circ Physiol. 303: H619–H628. Epub 2012/07/11.

Nederveen AJ, Avril S, Speelman L. 2014. MRI strain imaging of the carotid artery: present limitations and future challenges. J Biomech. 47:824–833. Epub 2014/01/29.

Nieuwstadt HA, Akyildiz AC, Speelman L, Virmani R, van der Lugt A, van der Steen AF, Wentzel JJ, Gijsen FJ. 2012. The influence of axial image resolution on atherosclerotic plaque stress computations. J Biomech. 46:689–695. Epub 2012/12/25.

Nieuwstadt HA, Geraedts TR, Truijman MT, Kooi ME, van der Lugt A, van der Steen AF, Wentzel JJ, Breeuwer M, Gijsen FJ. 2013. Numerical simulations of carotid MRI quantify the accuracy in measuring atherosclerotic plaque components *in vivo*. Magn Reson Med. 72:188–201. Epub 2013/08/15.

Nieuwstadt HA, Speelman L, Breeuwer M, van der Lugt A, van der Steen AF, Wentzel JJ, Gijsen FJ. 2013. The influence of inaccuracies in carotid MRI segmentation on atherosclerotic plaque stress computations. J Biomech Eng. 136, 021015. Epub 2013/12/10.

Ohayon J, Finet G, Gharib AM, Herzka DA, Tracqui P, Heroux J, Rioufol G, Kotys MS, Elagha A, Pettigrew RI. 2008. Necrotic core thickness and positive arterial remodeling index: emergent biomechanical factors for evaluating the risk of plaque rupture. Am J Physiol Heart Circ Physiol. 295: H717–H727. Epub 2008/07/01.

Ohayon J, Mesnier N, Broisat A, Toczek J, Riou L, Tracqui P. 2012. Elucidating atherosclerotic vulnerable plaque rupture by modeling cross substitution of ApoE-/-mouse and human plaque components stiffnesses. Biomech Model Mechanobiol. 11:801–813. Epub 2011/10/12.

Riou LM, Broisat A, Ghezzi C, Finet G, Rioufol G, Gharib AM, Pettigrew RI, Ohayon J. 2014. Effects of mechanical properties and atherosclerotic artery size on biomechanical plaque disruption – mouse vs. human. J Biomech. 47:765–772. Epub 2014/02/05.

Schroder J, Brinkhues S. 2014. A novel scheme for the approximation of residual stresses in arterial walls. Arch Appl Mech. 84:881–898.

Speelman L, Akyildiz AC, den Adel B, Wentzel JJ, van der Steen AF, Virmani R, van der Weerd L, Jukema JW, Poelmann RE, van Brummelen EH, Gijsen FJ. 2011. Initial stress in biomechanical models of atherosclerotic plaques. J Biomech. 44: 2376–2382.

Tang D, Yang C, Kobayashi S, Zheng J, Woodard PK, Teng Z, Billiar K, Bach R, Ku DN. 2009. 3D MRI-based anisotropic FSI models with cyclic bending for human coronary atherosclerotic plaque mechanical analysis. J Biomech Eng. 131, 061010. Epub 2009/05/20.

Tearney GJ, Regar E, Akasaka T, Adriaenssens T, Barlis P, Bezerra HG, Bouma B, Bruining N, Cho JM, Chowdhary S, et al. 2012. Consensus standards for acquisition, measurement, and reporting of intravascular optical coherence tomography studies: a report from the International Working Group for Intravascular Optical Coherence Tomography Standardization and Validation. J Am Coll Cardiol. 59:1058–1072. Epub 2012/03/17.

Teng Z, Sadat U, Li Z, Huang X, Zhu C, Young VE, Graves MJ, Gillard JH. 2010. Arterial luminal curvature and fibrous-cap thickness affect critical stress conditions within atherosclerotic plaque: an *in vivo* MRI-based 2D finite-element study. Ann Biomed Eng. 38:3096–3101. Epub 2010/05/26.

Vengrenyuk Y, Cardoso L, Weinbaum S. 2008. Micro-CT based analysis of a new paradigm for vulnerable plaque rupture: cellular microcalcifications in fibrous caps. Mol Cell Biomech. 5:37–47. Epub 2008/06/06.

Virmani R, Burke AP, Farb A, Kolodgie FD. 2006. Pathology of the vulnerable plaque. J Am Coll Cardiol. 47:C13–C18. Epub 2006/04/25.

von Birgelen C, Klinkhart W, Mintz GS, Papatheodorou A, Herrmann J, Baumgart D, Haude M, Wieneke H, Ge J, Erbel R. 2001. Plaque distribution and vascular remodeling of ruptured and nonruptured coronary plaques in the same vessel: an intravascular ultrasound study *in vivo*. J Am Coll Cardiol. 37:1864–1870. Epub 2001/06/13.

Williamson SD, Lam Y, Younis HF, Huang H, Patel S, Kaazempur-Mofrad MR, Kamm RD. 2003. On the sensitivity of wall stresses in diseased arteries to variable material properties. J Biomech Eng. 125:147–155. Epub 2003/03/29.